

**Computational Investigations into the
Structure and Reactivity of Small
Transition Metal Clusters**

by

Matthew Addicoat

B.Sc(Hons),
University of Adelaide, 2003

Thesis submitted for the degree of

Doctor of Philosophy

in

Chemistry
University of Adelaide

2009

© 2009
Matthew Addicoat
All Rights Reserved



Contents

Contents	iii
Abstract	vi
Statement of Originality	vii
Acknowledgements	viii
Publications	x
List of Figures	xi
List of Tables	xiii
Introduction	xvi
Chapter 1. Reactivity of TM Trimers with Carbon Monoxide: M_3CO	1
1.1 Introduction	2
1.2 Computational Method	4
1.3 Results and Discussion	6
1.3.1 Niobium, Molybdenum and Technetium	7
1.3.2 Ruthenium and Rhodium	12
1.3.3 Palladium and Silver	16
1.3.4 From Nb_3 to Ag_3 : Periodic Trends	19
1.3.5 Conclusion	24

Chapter 2. Better than DFT? Multireference calculations on TM clusters.	25
2.1 Nb ₃	26
2.1.1 Nb ₃	26
2.1.2 Nb ₃ ⁺	30
2.1.3 IP Calculations	33
2.2 Nb ₃ N ₂	35
2.2.1 Nb ₃ N ₂	35
2.2.2 Nb ₃ N ₂ ⁺	42
2.2.3 IP Calculations	46
2.3 Nb ₃ C ₂	48
2.3.1 Nb ₃ C ₂	48
2.3.2 Nb ₃ C ₂ ⁺	55
2.3.3 IP Calculations	59
2.4 Conclusions	61
 Chapter 3. The IP Problem: BFW	 62
3.1 Method	64
3.2 Results and Discussion	67
 Chapter 4. Structure Determination Using a Stochastic Search: Kick	 75
4.1 NbMoRuRhPd	80
4.2 Rh ₆	82
4.3 Pd _n Au _m (m + n = 5)	84
4.4 Nb _m Rh _n (m + n = 5)	89
 Chapter 5. Constraining a Stochastic Search with Molecular Fragments: Kick	 94
II	94
5.1 Introduction	95

5.2	Zeise's anion	97
5.3	Au_6 , $Au_6 + CO$, $Au_6 + O_2$, $Au_6 + CO + O_2$	101
5.3.1	Au_6CO	102
5.3.2	Au_6O_2	102
5.3.3	Au_6CO_3	104
5.4	Gly-Trp. nH_2O $n = 1,2$	110
Chapter 6. Changing cluster properties, one atom at a time: Nb_3X		117
6.1	Introduction	118
6.2	Computational Method	120
6.3	Results and Discussion	122
6.3.1	Bare Clusters	122
6.3.2	CO and C, O bound clusters	124
6.4	Conclusion	127
Conclusions		133
Appendix A. Nb_3X_2 orbitals		136
Appendix B. Kick Source Code		146
B.1	Kick-start	147
B.2	Kick-parse	151
B.3	Kick-freq	154
Appendix C. Supplementary Information		158
References		159

Abstract

This thesis presents a number of largely independent forays into developing an understanding of the unique chemistry of transition metal clusters. The first chapter of this thesis represents an initial foray into mapping the chemical reactivity of transition metal clusters - a monumental task that will doubtless continue for some time. The small slice undertaken in this work investigates the reactivity with CO of a series of the smallest possible metal clusters; $4d$ (Nb - Ag) homonuclear metal trimers. In Chapter 2, two known transition metal clusters were studied using CASSCF (MCSCF) and MRCI methods, only to find that DFT methods provided more accurate Ionisation Potentials (IPs) . Thus Chapter 3 was devoted to optimising a density functional to predict IPs. As clusters get larger, the number of possible structures grows rapidly too large for human intuition to handle, thus Chapter 4 is devoted to the use of an automated stochastic algorithm, "Kick", for structure elucidation. Chapter 5 improves on this algorithm, by permitting chemically sensible molecular fragments to be defined and used. Chapter 6 then comes full circle and uses the new Kick algorithm to investigate the reaction of CO with a series of mono-substituted niobium tetramers (i.e. Nb_3X) .

Statement of Originality

This work contains no material that has been accepted for the award of any other degree or diploma in any university or other tertiary institution and, to the best of my knowledge and belief, contains no material previously published or written by another person, except where due reference has been made in the text.

I give consent to this copy of the thesis, when deposited in the University Library, being available for loan, photocopying and dissemination through the library digital thesis collection.

Signed

Date

Acknowledgements

Science is an imaginative adventure of the mind seeking truth in a world of mystery. -

Sir Cyril Herman Hinshelwood (1897-1967) Nobel prize 1956.

I'm not entirely certain what Greg will think of being likened to an adventure tour guide, however, I thank him for his boundless enthusiasm, intuitive (yet subtle) guidance and all the rope he gave me. Particularly the rope. The work contained in this thesis (plus several false starts and interesting diversions) began with no more specific aim than using computational methods to "investigate the structure and properties of transition metal clusters", I enjoyed and greatly benefited from the freedom of direction implicit in such a broad project, however, it would not have been possible if it weren't for Greg's oversight.

I also thank my co-supervisor Mark Buntine, for pointing out several computational and technical errors. Sometimes even before I made them.

- None of the work contained in this thesis would have been possible without the support of the technical staff at the South Australian Partnership for Advanced Computing (SAPAC) and the Australian Partnership for Advanced Computing (APAC). In particular I would like to thank Patrick Fitzhenry and Grant Ward from SAPAC and Rika Kobayashi from APAC.
- While he has now moved on to greener and grassier pastures, Jeff Borkent, as the local computing officer in the chemistry department was invaluable.
- The chemistry librarian, Jane Wannan, who prevented me from wasting a great deal of time accessing obscure journal articles.
- My colleagues in the Laser Chemistry group at the University of Adelaide for all possible permutations of science, caffeine and beer.

- The work in Chapter 3 was undertaken in the research group of Peter Gill at the ANU. His guidance and wisdom as well as that of Andrew Gilbert was invaluable. This work was supported by a Mutual Community Postgraduate Travel Grant.
- The laptop that has been my best friend throughout my candidature was purchased with the aid of a Doreen McCarthy bursary.
- Deb Crittenden for being a source of moral, scientific and pseudo-random support as well as reading early drafts of Chapter 2.
- My family.
- Finally the \LaTeX template used to prepare this thesis is based on the template published by the Department of Electrical and Electronic Engineering, University of Adelaide.

Publications

Work contained in this thesis has appeared in the following publications:

- Pedersen, D. B.; Rayner, D. M.; Simard, B.; Addicoat, M. A.; Buntine, M. A.; Metha, G. F.; Fielicke, A.; Photoionization of Nb_3CO and $\text{Nb}_3(\text{CO})_2$: Is CO Molecularly or Dissociatively Adsorbed on Niobium? *J. Phys. Chem. A* **2004**, *108*, 964
- Addicoat, M. A.; Buntine, M. A.; Metha, G. F.; Gilbert, A. T. B.; Gill, P. M. W.; BFW: A Density Functional for Transition Metal Clusters *J. Phys. Chem. A* **2007**, *111*, 2628
- Addicoat, M. A.; Buntine, M. A.; Yates, B.; Metha, G. F.; Associative and Dissociative Binding of CO to 4d Transition Metal Trimers: A DFT Study *J. Comput. Chem.* **2008**, *29*, 1497
- Addicoat, M. A.; Metha, G. F.; Computational study of CO reactivity with Nb_3X heteronuclear clusters *Aust. J. Chem.* **2008**, *61*, 854
- Addicoat, M. A.; Metha, G. F.; Kick: Constraining a Stochastic Search Procedure with Molecular Fragments *J. Comput. Chem.* **2009**, *30*, 57

In addition, work undertaken during my candidature but not contained in this thesis has appeared in the following publications:

- Dryza, V.; Addicoat, M. A.; Gascooke, J. R.; Buntine, M. A.; Metha, G. F.; Ionization Potentials of Tantalum-Carbide Clusters: An Experimental and DFT Study *J. Phys. Chem. A* **2005**, *109*, 11180
- Dryza, V.; Addicoat, M. A.; Gascooke, J. R.; Buntine, M. A.; Metha, G. F.; Threshold Photo-ionization and DFT Studies of the Niobium-Carbide Clusters Nb_3C_n ($n = 1-4$) and Nb_4C_n ($n = 1-6$) *J. Phys. Chem. A* **2008**, *112*, 5582.

List of Figures

I-1	Molecular Orbital Diagram for Carbon Monoxide	xviii
I-2	Model double-well potential	xxiii
1.1	Stationary points on the Nb ₃ + CO potential energy surface.	8
1.2	Stationary points on the Mo ₃ + CO potential energy surface.	10
1.3	Stationary points on the Tc ₃ + CO potential energy surface.	11
1.4	Stationary points on the Ru ₃ + CO potential energy surface.	13
1.5	Stationary points on the Rh ₃ + CO potential energy surface.	15
1.6	Stationary points on the Pd ₃ + CO potential energy surface.	18
1.7	Stationary points on the Ag ₃ + CO potential energy surface.	19
1.8	Plot of binding energies for interesting M ₃ CO structures.	20
<hr/>		
2.1	Geometry of Nb ₃	27
2.2	Doubly and triply bridged Nb ₃ X ₂ structures.	35
<hr/> <hr/>		
4.1	Possible connectivities and permutations for a tetratomic molecule.	76
4.2	Kick identified structures for NbMoRuRhPd	81
4.3	Kick identified structures for Rh ₆	83
4.4	Kick identified structures for Pd ₅	85
4.5	Kick identified structures for Pd ₄ Au.	85
4.6	Kick identified structures for Pd ₃ Au ₂	86

4.7	Kick identified structures for Pd ₂ Au ₃	87
4.8	Kick identified structures for PdAu ₄	88
4.9	Kick identified structures for Au ₅	88
4.10	Kick identified structures for Nb ₅	89
4.11	Kick identified structures for Nb ₄ Rh.	90
4.12	Kick identified structures for Nb ₃ Rh ₂	91
4.13	Kick identified structures for Nb ₂ Rh ₃	92
4.14	Kick identified structures for NbRh ₄	92
4.15	Kick identified structures for Rh ₅	93

5.1	Kick identified structures for [PtCl ₃ (C ₂ H ₄)] ⁻	98
5.2	Kick identified structures for [PtCl ₃ (C ₂ H ₄)] ⁻	100
5.3	Kick identified structures for Au ₆	101
5.4	Kick identified structures for Au ₆ CO.	103
5.5	Kick identified structures for Au ₆ O ₂	104
5.6	Kick identified structures for Au ₆ CO ₃	106
5.7	Structures of Gly-Trp.nH ₂ O n = 1,2.	116

6.1	Structures and relative energies (eV) of neutral and cationic Nb ₃ X clusters	129
6.2	Structures and relative energies (eV) of neutral Nb ₃ X-CO clusters	130
6.3	Structures and relative energies (eV) of neutral Nb ₃ X-C-O clusters	131

List of Tables

I-1	The effect of changing co-ordination site on ν_{CO}	xix
1.1	Energies of doublet Nb ₃ -CO structures.	8
1.2	Energies of singlet and triplet Mo ₃ -CO structures.	9
1.3	Energies of Tc ₃ -CO structures.	11
1.4	Energies of septet and nonet Ru ₃ -CO structures.	13
1.5	Energies of double, quartet and sextet Rh ₃ -CO structures.	14
1.6	Energies of singlet and triplet Pd ₃ -CO structures.	17
1.7	Energies of doublet Ag ₃ -CO structures.	19
1.8	Literature bond strengths for the transition metal oxides and carbides.	21
1.9	CO vibrational frequencies and change in π^* orbital energies for M ₃ CO capture species.	23
2.1	Geometric parameters, relative energies and vibrational frequencies of Nb ₃ at the B3LYP/srsc level.	28
2.2	Literature geometric parameters, relative energies and vibrational frequencies of Nb ₃ at the B3LYP/srsc level.	28
2.3	CASSCF geometric parameters and relative energies of electronic states of Nb ₃ at the CASSCF and MRCI levels.	29
2.4	Literature geometric parameters and relative energies of electronic states of Nb ₃ at the CASSCF and MRCI levels.	29
2.5	Assignment of the Photoelectron Spectrum of Nb ₃	30
2.6	Geometric parameters, relative energies and vibrational frequencies of Nb ₃ ⁺ at the B3LYP/srsc level.	31

2.7	CASSCF geometric parameters and relative energies of electronic states of Nb_3^+ at the CASSCF and MRCI levels.	32
2.8	Literature geometric parameters and relative energies of electronic states of Nb_3^+ at the CASSCF and MRCI levels.	32
2.9	Calculated IP of Nb_3 at the DFT and MRCI levels.	34
2.10	CASSCF geometric parameters and relative energies of electronic states of Nb_3N_2 at the CASSCF, MRCI and MRCI+Q levels.	38
2.11	Geometric parameters, relative energies and vibrational frequencies of Nb_3N_2 at the B3LYP/srsc level.	41
2.12	CASSCF geometric parameters and relative energies of electronic states of Nb_3N_2^+ at the CASSCF, MRCI and MRCI+Q levels.	43
2.13	Geometric parameters, relative energies and vibrational frequencies of Nb_3N_2^+ at the B3LYP/srsc level.	45
2.14	Calculated IP of Nb_3N_2 at the DFT and MRCI levels.	47
2.15	CASSCF geometric parameters and relative energies of electronic states of Nb_3C_2 at the CASSCF, MRCI and MRCI+Q levels.	51
2.16	Geometric parameters, relative energies and vibrational frequencies of Nb_3C_2 at the B3LYP/sdd level.	54
2.17	Geometric parameters and relative energies of electronic states of Nb_3C_2^+ at the CASSCF, MRCI and MRCI+Q levels.	56
2.18	Geometric parameters, relative energies and vibrational frequencies of Nb_3C_2^+ at the B3LYP/sdd level.	58
2.19	Calculated IP of Nb_3C_2 at the DFT and MRCI levels.	60
2.20	Errors in calculated IPs of niobium clusters at the DFT and MRCI+Q levels.	61
3.1	The 26 transition metals in the training set.	71
3.2	The 21 dimers in the training set.	72

3.3	The five combinations of functionals with the lowest MAD.	73
3.4	MAD and MSD errors (eV) for the IPs of transition metal complexes.	73
3.5	Experimental and calculated frequencies (cm^{-1}) for clusters in the test set. . .	74
3.6	RMS thermochemical errors (kJ/mol) for functionals applied to the G2 dataset. . .	74
5.1	Energies of selected low-energy isomers of Au_6	102
5.2	Energies of selected low-energy isomers of Au_6CO	103
5.3	Energies of selected low-energy isomers of Au_6O_2	105
5.4	Energies of selected low energy isomers of Au_6CO_3	105
5.5	Energies of Gly-Trp. H_2O structures.	113
5.6	Energies of Gly-Trp. $(\text{H}_2\text{O})_2$ structures.	115
6.1	Adiabatic IPs and EAs of Nb_3X clusters.	128
6.2	Mulliken populations of Nb_3X clusters.	128
6.3	CO binding energies of Nb_3X clusters.	132
A.1	C_{2v} character table	137

Introduction

Stability, Structure and Reactivity of Metal Clusters

Intermediate between single molecules and bulk materials lie a class of materials termed clusters. A cluster is an aggregate of finite size, containing between 2 and 10^4 particles. These particles may be atoms or molecules. Transition metal clusters are aggregates of transition metal atoms that may or may not include the presence of main group elements integral to the cluster structure. M is used throughout this thesis to indicate a metal atom.

The electronic, geometric and chemical characteristics of materials depend not only on the state (solid, liquid, solution...), or phase of the material but the size as well. The study of cluster properties and behaviour provides us with a means to map the transition between single molecule phenomena and bulk or condensed phase phenomena [1].

There exist two distinct regimes for the mapping of size effects to an observable property:

1. *Large Clusters*

In the large cluster regime, evolution of bulk surface and matter properties occurs smoothly with increasing cluster size. Clusters in this regime typically contain hundreds or thousands of particles.

2. *Small Clusters*

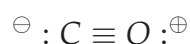
In the small cluster regime, observables such as electronic, magnetic and structural properties exhibit an irregular size dependence. It is in this regime where *magic – number* structures that exhibit particular or striking properties exist. These structures commonly possess extra stability lent by a closed atomic or electronic shell. Clusters that have at

least one dimension in the nanometre (10^{-9}m) regime and possess similar structure to that of the bulk are often termed *nanocrystals*.

Due to the remarkable variation in properties, it is the small cluster regime that is of most interest to researchers. Transition metal clusters and their reactions with various molecules serve as model systems for catalysis and surface science [2]. Small clusters exhibit striking differences in reactivities dependent upon cluster size, geometry and electronic structure.

Carbon Monoxide

Carbon monoxide is an unusual molecule. While oxygen is the more electronegative atom, it is the carbon that bears a δ^- charge. Experimentally, a dipole moment of 0.122 Debye is observed, leading to the following Lewis representation:



The following molecular orbital diagram better describes CO (Figure I-1). The relatively small difference in energy between the carbon 2s and the oxygen 2p orbitals ($(-19.4 \text{ eV} + 15.9 \text{ eV}) = (-)3.5 \text{ eV}$) means there is significant overlap between these orbitals. The 2s and 2p_z orbitals mix to form an sp hybrid σ -type orbital. Each of these has a large lone pair-like lobe centred on the one atom, pointing outward and a small lobe directed towards the other atom [3]. Note that only the p_z orbital is of the correct symmetry to overlap with an s-type orbital. The 4 σ orbital is closer in energy to oxygen and thus centred on oxygen, while the 5 σ is centred on the carbon atom. These “lone pair” orbitals are both weakly bonding .

As carbon monoxide has 10 valence electrons (four from carbon and six from oxygen), orbitals up to and including 5 σ are filled. It is thus the lone pair on carbon that is the Highest Occupied

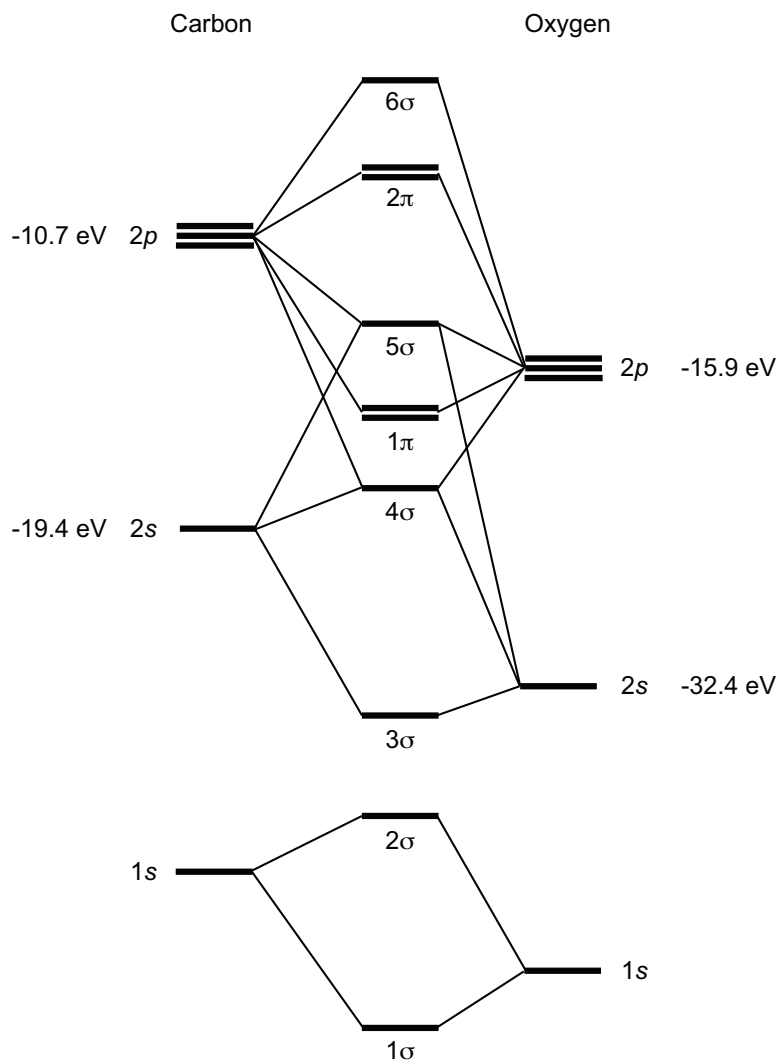


Figure I-1: Molecular Orbital diagram for carbon monoxide

Molecular Orbital (HOMO) of carbon monoxide. This lone pair is responsible for the Lewis base properties of carbon monoxide.

The Lowest Unoccupied Molecular Orbital (LUMO) of carbon monoxide are the 2 π orbitals. These orbitals lie closer to carbon than oxygen and are relatively low in energy. These orbitals are antibonding in character and are able to accept electron density, resulting in the Lewis acid properties of carbon monoxide.

Both the Lewis acid and Lewis base characteristics of carbon monoxide are important in describing its binding to a metal species. Initially donation from the HOMO of carbon monoxide, the 5σ (carbon lone pair) orbital to the metal occurs. Once the sigma bond is established, π donation from the d-orbitals of the metal into the 2π antibonding orbitals of carbon monoxide occurs. This phenomena is commonly called *back-bonding*. Thus the metal-carbon bond is strengthened at the expense of the carbon-oxygen bond which is weakened. The extent of π back-bonding can be determined from the frequency of the C-O stretch. It is expected that a greater degree of back-bonding will increase the electron density in the 2π antibonding orbital of carbon monoxide. The formal bond order of the C-O bond is thus reduced, leading to a longer bond and a lower stretching frequency.

Given the direct link between the extent of metal \rightarrow carbon electron donation and ν_{CO} it can also be expected that the CO stretching frequency can differentiate between binding at different metal sites. To denote different co-ordination sites, μ notation is used. μ^1 indicates binding atop a single atom. μ^2 indicates binding with two metal centres (across a bond), i.e.. doubly bridging and likewise, μ^3 indicates the ligand is triply bridging. Remembering the frequency of free CO, $\nu_{\text{CO}} = 2143 \text{ cm}^{-1}$, the following trend can be observed [4] (Table I-1).

Bond Type	ν_{CO} (cm^{-1})
Terminal or atop, M-CO (μ^1)	2125-1850
Doubly bridging: μ^2	1850-1750
Triply bridging: μ^3	1675-1750

Table I-1: The effect of changing co-ordination site on ν_{CO} .

Many studies involving the carbon monoxide molecule have focussed on its utility as a probe, the reduction in carbonyl stretching frequency indicating the strength of $M_n - \text{CO}$ interaction. Carbonyl frequency however, is not a linear guide to surface site selection [5]. The observed metal-carbon monoxide bonding is affected by the ability of the metal to mix s - and d -type orbitals, which favours participation of these orbitals in both σ and π bonding. Mixing is expected to lower the initial σ repulsion and provide orbital energies suitable for back-donation

to carbon monoxide, (π).

Thus it is expected that the binding characteristics of $M_n\text{CO}$ will be determined not only by the electronic configuration and energetics of the metal atoms involved but also by the metal-metal bonding framework and the geometric sites available on the cluster.

Transition Metals as Catalysts

Transition metals are uniquely active as catalysts and enjoy widespread use in industrial processes. Their activity is generally attributed to the d -electrons that occupy a band near the Fermi level. These d -electrons, particularly when they mix with s - and p - type orbitals to form hybridised orbitals, give rise to a large number of nearly degenerate, low-lying electronic states and empty electronic orbitals. This high density of electronic states is ideal for catalysis; surface sites with a high density of electronic states that can accept or donate electrons are the most active in forming and breaking chemical bonds.

It is expected that as the number of d -electrons increases moving from left to right across the Periodic Table, the population of the antibonding orbitals increases as the bonding orbitals are already filled. Therefore, metals to the left of the Periodic Table form stronger metal-adsorbate chemical bonds than those metals to the right of the Periodic Table. Heats of chemisorption of carbon monoxide on various transition metal surfaces [6] indicate that those metals which chemisorb carbon monoxide more strongly than iron (i.e. to the left of iron) will dissociate carbon monoxide, while those metals that chemisorb carbon monoxide less strongly than iron (i.e. to the right of iron) will not dissociate carbon monoxide.

In order to design high efficiency and high selectivity transition metal catalysts, it is desirable to tune the amount of electron density at the metal centres. Fine tuning of the transition

metal electron density allows control of the adsorbate bond order by precise population of the adsorbate antibonding orbitals. Transition metal electron density can be altered in three main ways; (1), by explicitly charging the surface; (2), by the addition of other ligands that are electron donating or withdrawing, or (3), by introducing surface defects. Surface defects cause large changes in the local density of electronic states which correlate with catalytic activity. Small transition metal clusters contain a high proportion of edge and corner atoms that can be considered analogous to bulk surface defects. It is thus plausible to tailor a small transition metal cluster for use as an active catalyst.

The adoption of clusters as catalytic systems is made difficult however, by the difficulty in characterising clusters. The seemingly random variation of properties and reactivities with cluster size in small transition metal clusters cannot be explained simply. Rayner *et al* [7] measured the absolute rate coefficients for the reaction of niobium clusters, Nb_n , with N_2 and D_2 and found large, seemingly random variations in the measured coefficients with conspicuous (three orders of magnitude!) local minima in reactivity being observed at Nb_8 , Nb_{10} and Nb_{16} . These local minima coincide with local maxima in Ionisation Potential (IP) and thus a simple correlation between charge transfer ability and reactivity was proposed [8]. Unfortunately, no globally consistent correlation between IP and reactivity of niobium clusters exists [9]. Adding to the evidence against a simple charge transfer model is that the cluster cations and anions have been shown to exhibit similar reactivity to the neutral species [10].

Thus it seems that geometric structure is an important factor in controlling reactivity. Experiments undertaken by Morse *et al.* [11] and Smalley *et al.* [12] have indicated the presence of structural isomers in neutral and charged niobium clusters. These isomers were shown to have different reactivities toward N_2 and D_2 , further supporting the role of geometric structure in cluster reactivity and reinforcing the idea of tailoring transition metal clusters for use as efficient and specific catalysts.

Recent studies by Ervin *et al.* [13] and Heiz *et al.* [14–17] have illustrated the capacity for a full thermal catalytic cycle to occur on a metal cluster. Ervin *et al.* have illustrated two such examples for the oxidation of carbon monoxide to carbon dioxide using gas phase Pt_n , ($n=3-6$) clusters in a flow tube apparatus at room temperature. Heiz *et al.* used small Pd_n , ($n \leq 30$) clusters adsorbed on an MgO surface to catalyse the $2CO + 2NO \rightarrow N_2 + 2CO_2$ reaction at 300 K, which is 150 K lower than the crystal surface reaction.

This observed complex and vast variation in behaviour yields quite an exciting challenge in its own right for cluster chemists and there is a great deal of work to be done in order to determine general rules that may predict cluster reactivity. Clusters share some characteristics with their bulk analogues but maintain notable differences. Elucidation of the similarities and differences between clusters and bulk transition metals and how these steric and electronic factors determine chemical reactivity is a vastly important endeavour.

Double-well Model

Considering only a single cluster + molecule reaction, allows the problem to be phrased in more direct terms. The reaction of a small molecule with a transition metal cluster proceeds by a number of key steps: Firstly an intact small molecule approaches the cluster and binds, then it may or may not rearrange prior to possible dissociation.

Thus there are a relatively small number of key questions one might ask about a small molecule binding to a transition metal cluster, namely: What is the depth of the well in which the lowest energy associatively bound species (which may or may not be the initial or 'capture' species) resides? What is the depth of the well corresponding to the lowest energy dissociatively bound species? How high is the barrier between these two wells? Answers to these questions may be effectively represented by a double-well potential, which in turn represents a vastly simplified

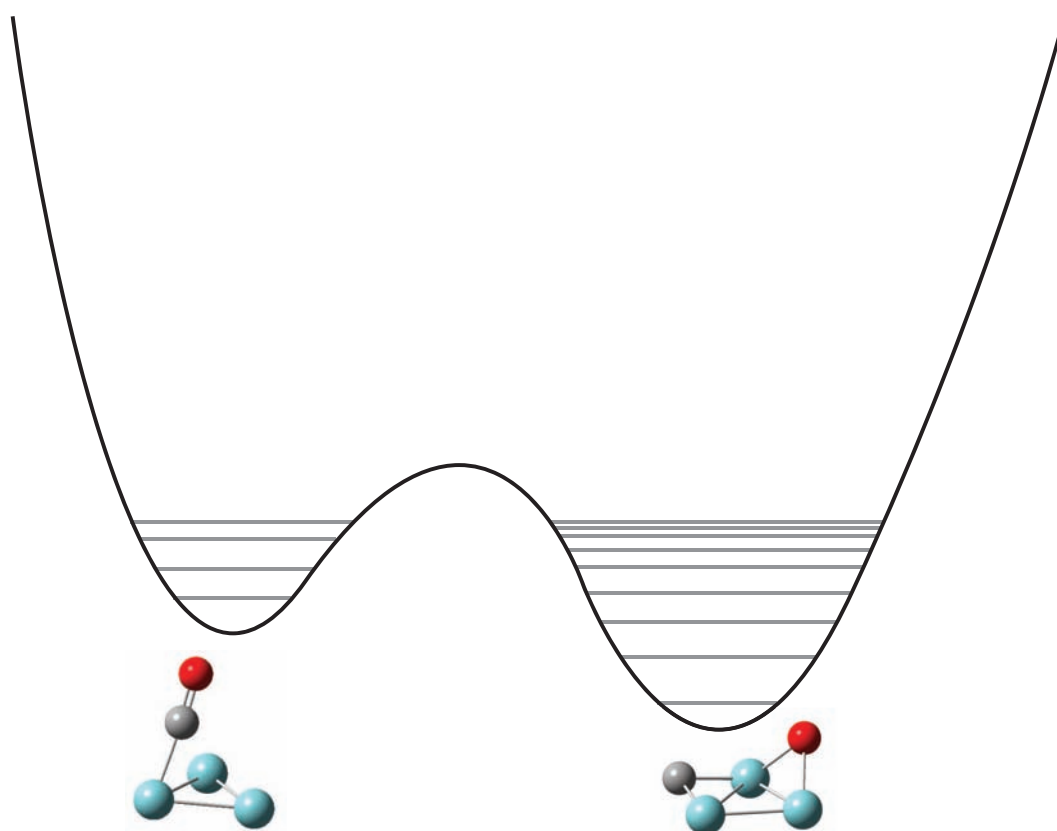


Figure I-2: Model double-well potential with an arbitrary energy scale (vertical axis). Associatively and dissociatively bound M_3CO structures are indicated at the bottom.

Potential Energy Surface (PES) for the reaction.

The Problems with Spectroscopic Probing

Probing transition metal clusters, in order to gain structural information has proved more difficult than their manufacture. Nonadiabatic behaviour, resulting from large numbers of vibrational degrees of freedom and many low-lying electronic states mean that typical laser based spectroscopic techniques such as REMPI (Resonance Enhanced MultiPhoton Ionisation) and LIF (Laser Induced Fluorescence) are ineffective [18].

An example of the difficulties encountered in applying traditional techniques to multiple transition metal containing systems is provided by comparing TiO and Nb₂: In the first 4 eV, TiO has 21 stable electronic states, Nb₂ on the other hand has 120. The near continuum of low lying electronic states make spectroscopies that rely on electronic excitation, such as REMPI and LIF, difficult to use.

An interesting feature of many transition metal clusters, that further complicates analysis, is their fluxional nature. A pseudorotation barrier of less than 0.04 kJmol⁻¹ has been reported for the neutral niobium trimer [19]. Multi-reference studies undertaken by Balasubramanian *et al.* indicate a similarly small barrier for the rhodium trimer [20].

It has subsequently proved difficult to fully characterise clusters containing more than a few metal atoms. Some of the largest systems to be fully characterised by both spectroscopic and theoretical means are the neutral and cationic forms of Nb₃O, Nb₃N₂ and Nb₃C₂ [21–24] which were studied using Pulsed Field Ionisation-Zero Electron Kinetic Energy spectroscopy (PFI-ZEKE) and DFT (B3P86) methods. A related method, Mass-Analysed Threshold Ionisation (MATI) is also gaining prominence as a spectroscopic method coupled to a molecular beam experiment. MATI has the advantage of mass selection, which allows the parent ion to be determined by its mass-charge ratio. Both of these techniques rely on ionisation, with detection based on TOF-MS. Some more direct structural information can be gained by IR-Multiphoton Ionisation (IR-MPI) experiments in which a tuneable infrared free electron laser is used to excite clusters such that they undergo delayed ionisation. Ionisation is enhanced when the laser wavelength matches a vibrational resonance within the cluster. This experiment was used to determine that CO dissociates on small niobium clusters [25], but remains intact on small rhodium clusters [26].

Except in these rare cases, it is challenging to even determine the basic ‘signposts’ characterising a cluster reaction, such as whether associative or dissociative binding occurs, the depth of these wells and the barrier between them (adopting the double-well model above). Hence many studies employ computational methods to both guide experimental exploration and to elucidate the results of experiments.

In particular, computational methods used in conjunction with appropriate spectroscopic techniques are proving invaluable as aids to structure determination. *Ab initio* and DFT calculations can be carried out to determine molecular configurations consistent with observed spectra [27, 28]. Computational prediction of cluster properties (such as ionisation potentials) is also employed prior to experimental work to determine species that may be observable by a given experiment.

The computational chemist has a number of tools at their disposal to meet these challenges and to complement experimental approaches. The following section gives a brief introduction to the key components of this toolkit.

Computational Chemistry

“The underlying laws necessary for the mathematical theory of a large part of physics and the whole of chemistry are thus completely known, and the difficulty is only that the exact application of these laws leads to equations much too complicated to be soluble.”

- P.A. Dirac, 1929

The ultimate goal of quantum chemical calculations is the solution of the time-independent, non-relativistic Schrödinger equation:

$$\hat{H}\Psi(\vec{x}_1, \vec{x}_2 \dots \vec{x}_N, \vec{R}_1 \vec{R}_2 \dots \vec{R}_M) = E\Psi(\vec{x}_1, \vec{x}_2 \dots \vec{x}_N, \vec{R}_1 \vec{R}_2 \dots \vec{R}_M) \quad (I-1)$$

for a system of N electrons and M nuclei. In the above equation, \hat{H} is the Hamiltonian operator that represents the total energy, Ψ is the wavefunction and E is the energy of the particle. Solutions to this equation represent *stationary points* on the multidimensional potential energy surface of the molecule. The potential energy surface for a molecule has $3N - 6$ degrees of freedom or for linear molecules $3N - 5$, where N is the number of atoms. This number corresponds to freedom along each of the three cartesian axes (x, y, z) for each atom subtract three degrees which correspond to translation of the entire molecule along each of the three axes and subtract another three degrees for rotation of the entire molecule about each of the three axes. For linear molecules rotation about either of the non-molecular axes is equivalent. The remaining degrees of freedom correspond to vibrations, where some or all atoms move in a co-ordinated, often characteristic fashion whilst preserving the centre of mass of the molecule as a whole.

Frequency calculations are undertaken on all stationary point geometries found to determine their nature. For chemical systems solutions with either zero or one imaginary frequency are sought. Solutions that possess no imaginary frequencies correspond to minima on the potential energy surface. To perturb the geometry in any way, raises the energy of the molecule. Solutions with one imaginary frequency correspond to transition states, the lowest energy configuration linking two minima.

To determine the minima connected by a transition state, Intrinsic Reaction Co-ordinate (IRC) calculations can be undertaken. The IRC is defined as the steepest descent path from the transition state in mass-weighted cartesian co-ordinates.

Variational Principle

In reality, for all bar a few chemically trivial cases there is no strategy to analytically solve the Schrödinger equation to obtain the exact wavefunction. There is however a recipe for

systematically approaching the ground state wavefunction, Ψ_0 .

The energy computed as the expectation value of the Hamiltonian operator \hat{H} from any guessed wavefunction, Ψ_{trial} will be an *upper bound* to the true energy of the ground state.

i.e.:

$$\langle \Psi_{trial} | \hat{H} | \Psi_{trial} \rangle = E_{trial} \geq E_0 = \langle \Psi_0 | \hat{H} | \Psi_0 \rangle \quad (I-2)$$

Note that it is possible (though highly unlikely!) to correctly guess Ψ_{trial} in which case the above equality holds.

So now all one has to do is search through all acceptable N-electron wavefunctions. An acceptable wavefunction must be continuous over all space and be quadratically integrable (or else normalisation is not possible). Searching through *all* acceptable wavefunctions is not feasible. A subset of wavefunctions is chosen to search. Most subsets are chosen to allow the minimisation algorithm to follow some well-defined algebraic scheme until a target minimum energy is attained.

$$E_0 = \min_{\Psi \rightarrow N} E[\Psi] = \min_{\Psi \rightarrow N} \langle \Psi | \hat{T} + \hat{V}_{Ne} + \hat{V}_{ee} | \Psi \rangle \quad (I-3)$$

The Born-Oppenheimer Approximation

The quest for an approximate solution to the Schrödinger equation is made a lot easier and less expensive if we take advantage of the fact that nuclei are many orders of magnitude more massive than electrons. Due to this large difference in mass, electrons can be considered to move instantaneously with respect to the timescale required to effect nuclear motion. We can thus treat the system as a set of fixed nuclear co-ordinates with electrons given free movement within the system. This is the Born-Oppenheimer or *clamped-nuclei* approximation.

Because the nuclei are fixed, their kinetic energy is zero and nuclear-nuclear repulsion is constant, thus the full Hamiltonian reduces down to the electronic Hamiltonian:

$$\hat{H}_{elec}\Psi_{elec} = E_{elec}\Psi_{elec} \quad (1-4)$$

where Ψ_{elec} is the electronic wavefunction and E_{elec} is the electronic energy. The total energy, E_{total} , of the system is thus:

$$E_{total} = E_{nuc} + E_{elec} \quad (1-5)$$

where E_{nuc} is given by the expression:

$$E_{nuc} = \sum_{A=1}^M \sum_{B>A}^M \frac{Z_A Z_B}{r_{AB}} \quad (1-6)$$

Wavefunction Based Methods

As previously stated, unfortunately for chemists, there exists no strategy to exactly solve the Schrödinger equation for atomic or molecular systems. There is however a way to systematically approach the ground state wavefunction, Ψ_0 . Remembering the variational principle:

$$\langle \Psi_{trial} | H | \Psi_{trial} \rangle = E_{trial} \geq E_0 = \langle \Psi_0 | H | \Psi_0 \rangle \quad (1-7)$$

To determine the ground state wavefunction then only requires searching through all possible N-electron wavefunctions to find the one that yields the lowest energy. In practice, this is not feasible and so a subset of functions is generally chosen to search through, the result will be the ground state wavefunction within the chosen subset.

One of the most common approximations made, is the Hartree-Fock approximation, which assumes that the N-electron wavefunction can be composed as the antisymmetrised product of N one-electron wavefunctions or spin orbitals. In the Hartree-Fock approximation, each spin

orbital is optimised within the average field of the other $N-1$ electrons, i.e. electron-electron repulsion is entirely neglected by Hartree-Fock theory. Hartree-Fock wavefunctions thus tend to allow electrons to be too close together, increasing the electron-electron repulsion and thus raising the energy. The difference between the Hartree-Fock ground state energy and the true ground state energy is termed the correlation energy and may be understood as the effect of electrons interacting with each other. For accurate energetics, it is necessary to recover the correlation energy. Common methods for including electron correlation effects are:

Moller-Plesset (MP n) perturbation theory treats correlation as a perturbation to the zero-th order Hamiltonian. The number, n , refers to the truncation of the power series expansion. MP2, MP3 and MP4 are commonly used, higher orders are possible but rarely implemented due to their computational expense.

Multi-Configuration SCF (MCSCF) improves on SCF by optimising the orbitals for a combination of configurations. A calculation that included all possible electronic configurations would be called a Complete Active Space SCF (CASSCF) calculation. This is prohibitively expensive and so most calculations select a subset of orbitals that electrons may be excited into and freeze the core orbitals. Restricted Active Space (RAS) calculations like this often denote the active space in brackets, i.e. (m,n) for a calculation placing m electrons in n orbitals. The choice of active space can only be made with knowledge of the chemistry that one is investigating.

Configuration Interaction (CI) methods, generate excited configurations from either a single or multiple reference wavefunction. Full CI, which corresponds to every possible excited configuration is far too expensive for all but the smallest of molecule / basis set combinations and so common approximations are limiting to only singly excited configurations; CI-Singles or

CIS doubly excited configurations, CID or both singly and doubly excited configurations, CISD.

Finally, Coupled Cluster (CC) methods also generate excitations from a reference wavefunction. Unlike CI methods, the formalism of the CC theory guarantees size-consistency. The same abbreviations for included excitations are used, i.e. CCSD includes single and double excitations, CCSD(T) includes single and double excitations and includes the effect of triple excitations using perturbation theory, CCSDTQ includes single, double, triple and quadruple excitations.

All of these methods are computationally expensive, limiting the size of systems that can be treated. While Hartree-Fock theory scales as N^4 , MP2 scales as N^5 , MP4 scales as N^7 , CCSD scales as N^6 and CCSDT scales as N^8 , where N is the number of basis functions.

Density Functional Theory

An alternate and often complementary approach to wavefunction based methods for approximately solving the Schrödinger equation lies in Density Functional Theory or DFT. Density functional theory was independently derived by both Thomas [29] and Fermi [30–32] in the 1920's but it was some nearly 40 years until a series of papers appeared in the Physical Review [33–35]. These papers provided a firm theoretical basis for the use of the electron density as the basic variable in computational chemistry as well as a formal algorithmic implementation.

Despite the long history of DFT, it has only been in the most recent decade that it has become useful to the computational chemist. Indeed, in the first implementation of the Thomas-Fermi model, no system was stable with respect to its fragments [36]. No wonder chemists didn't want to use a model where chemical bonding couldn't exist! It wasn't until Kohn and Sham introduced the idea of combining an orbital based approach with a universal density functional

approach for a practical implementation of DFT to be useful for computational chemists.

DFT has several advantages over wavefunction based methods, firstly while Hartree-Fock theory has made and provided for large advances in solving many chemistry problems, it is limited by its initial assumption that the N -electron wavefunction can be represented by N one-electron wavefunctions. Inaccuracies generated by this initial assumption can be somewhat alleviated by combining several Slater determinants but for high accuracy methods as many as 10^9 determinants may be required, making the calculation not only computationally expensive but difficult for the human chemist to comprehend. DFT in principle makes no such initial assumption and is in principle exact.

The DFT approach is somewhat easier to comprehend, rather than basing calculations on a truncated Hilbert space of single-particle orbitals, the central variable is the real, physical electron density, in cartesian space that surrounds the molecule of interest.

The final advantage is computational expense. Practically, a typical implementation scales with $O(m^\alpha)$ with $2 \leq \alpha \leq 3$ [37] allowing accurate treatment of 'large' systems within reasonable computer time. O is used to indicate *Order*, the formal mathematical way of indicating scaling. For comparison, formal Hartree-Fock scales as $O(m^4)$, Second-order Moller-Plesset theory scales as $O(m^5)$ and both QCISD(T) and CCSD(T) scale as $O(m^7)$ [36].

The Hohenberg-Kohn Theorems

First Hohenberg-Kohn Theorem

To give DFT a firm theoretical basis, the assumption that the ground state potential is directly related to the ground state electron density needs to be proven. Importantly, no two possible

electron densities should lead to the same potential. This is proved by the first Hohenberg-Kohn theorem, which is stated formally below:

"The external potential $V_{ext}(\vec{r})$ is (to within a constant) a unique functional of $\rho(\vec{r})$; since in turn $V_{ext}(\vec{r})$ fixes \hat{H} we see that the full many body particle ground state is a unique functional of $\rho(\vec{r})$ " [33]

The proof of this statement is a reductio ad absurdum.

Second Hohenberg-Kohn Theorem: Variational Principle

The first Hohenberg-Kohn theorem proved that using the electron density as the basic variable was physically sound. The second theorem, presented in their landmark 1964 paper underlines this soundness, proving that the Hohenberg-Kohn functional, $F_{HK}[\rho]$ will return the lowest energy if and only if $\rho = \rho_0$.

This is effectively the variational principle in disguise, mathematically:

$$E_0 \leq E[\tilde{\rho}] = T[\tilde{\rho}] + E_{Ne}[\tilde{\rho}] + E_{ee}[\tilde{\rho}] \quad (1-8)$$

i.e. For any given density $\tilde{\rho}(\vec{r})$ connected with some external potential \tilde{V}_{ext} and which meets the required boundary conditions such as $\tilde{\rho}(\vec{r}) \geq 0$ and $\int \tilde{\rho} d(\vec{r}) = N$ the energy given by the Hohenberg-Kohn functional is an upper bound to the true energy, E_0 of the system.

Kohn-Sham Approach

Given that the exact functional forms required to determine both the kinetic energy and the electron-electron repulsion contributions to the total energy are unknown it may be wondered how DFT can produce such accurate results [38–40]. Given the spectacular failure of the

initial Thomas-Fermi model to describe molecular bonding and the comparative success of the Hartree-Fock approach, Kohn and Sham sought a better way to describe the kinetic energy contribution [41].

The method employed in the Kohn-Sham scheme is to recognise that the Slater determinant used in the Hartree-Fock scheme, while an approximation to the true N-electron wavefunction, is an exact wavefunction for N non-interacting electrons and an energy computed using the wavefunction is the exact energy for a system of neutral fermions. It is thus possible to set up a *non-interacting reference system*, whose wavefunction is a single Slater determinant. Therefore, having computed the largest part of the kinetic energy exactly, it is left to compute the remainder, or the difference between the fictitious non-interacting system and the real, interacting one by approximate means.

To do this, Kohn and Sham separated the Hohenberg-Kohn functional as follows:

$$F[\rho(\vec{r})] = T_S[\rho(\vec{r})] + J[\rho(\vec{r})] + E_{XC}[\rho(\vec{r})] \quad (I-9)$$

where T_S is the kinetic energy of the non-interacting system, J represents the classical (Coulomb) interaction and E_{XC} represents the *exchange-correlation energy*.

The new term is the exchange-correlation energy, included in this term are the residual kinetic energy (i.e. that not covered by T_S), self-interaction correction, exchange and correlation. In short, E_{XC} is the functional that contains everything we do not know exactly.

In seeking to implement the above functional however, we note that while T_S does have an explicit, solvable form, it depends not on the electron density, ρ but on a set of orbitals that comprise our non-interacting reference system. In turn, these Kohn-Sham orbitals determine the ground state density. Thus, the Kohn-Sham scheme, like the Hartree-Fock SCF scheme

needs to be solved iteratively.

Exchange and Correlation Energies

Exchange (Fermi) energy

Exchange or Fermi interaction occurs between *electrons of parallel spin* and arises directly from the Pauli Principle which states that electrons of like spin cannot be found at the same point in space. Thus electrons of the same spin do not move independently of each other, they experience an effective "extra" repulsion which is not related to charge-charge or Coulomb repulsion.

This extra repulsion would occur equally between neutral fermions (electrons belong to the class of subatomic particles called fermions). In most cases Fermi effects dominate Coulomb effects.

Correlation (Coulomb) energy

Correlation (Coulomb) interaction occurs between electrons of anti-parallel spin and is due to mutual Coulombic repulsion.

Note that the term correlation energy is often used to refer to the quantity:

$$E_{corr} = E_{actual} - E_{Hartree-Fock}$$

This is due to the fact that standard HF theory fails to take into account any form of correlation, treating electrons as non-interacting. In this context the correlation energy is always a negative quantity because the Hartree-Fock energy is always an upper bound to the true energy and any further computation would lead to a lower energy (Variational Principle). A more physical interpretation is because HF theory treats electrons as non-interacting, it places them too close together, increasing the electron-electron repulsion and thus raising the energy. Finally, it can be seen that both Fermi and Coulomb interaction lead to an "exclusion zone"

around any chosen reference electron. This exclusion zone is termed the *exchange-correlation hole*.

There are two general approaches to calculation of the exchange and correlation energies within DFT methods. The first approach is to employ only the electron density and is termed a local method. The other approach is to employ both the electron density and the gradient of the electron density. This approach is termed either a gradient corrected method or Generalised Gradient Approximation (GGA). Both of these two approaches are “pure” DFT methods. It is possible and often desirable to combine DFT functionals with Hartree-Fock exchange energies. These *hybrid methods* benefit from the incorporation of HF exchange, which is calculated exactly.

Local Density Approximation (LDA) Method

The most commonly employed local functionals are the Slater exchange functional paired with the local VWN (Vosko, Wilk and Nusair) functional. This approach can be referred to either by its functional abbreviation SVWN or by the acronym LDA which stands for Local Density Approximation. In the open-shell, unrestricted case this method becomes the Local Spin Density Approximation or LSDA.

Gradient-Corrected Methods

Local (spin) density methods are only able to achieve modest accuracy. Indeed, when LDA was the only DFT method available, computational chemists mainly avoided DFT. The first logical step to improving the accuracy of the local density approximation was to not only include a term for the density but also a term describing the *gradient* of the charge density. Thus the local density approximation becomes the first term in a Taylor series expansion that takes into account the non-homogeneity of the true electron density.

Hybrid Methods

The mixture of exact HF exchange and approximate DFT exchange is commonly employed to increase performance. Several different mixing ratios have been advocated.

Becke Half-and-Half LYP uses a 1:1 ratio of HF and DFT exchange energies. i.e.:

$$E_{XC} = \frac{1}{2}E_X(HF) + \frac{1}{2}E_X(Becke88) + E_C(LYP)$$

The most commonly employed hybrid method is the Becke 3-parameter scheme (B3). The scheme is represented as follows:

$$E_{XC} = 0.2E_X(HF) + 0.8E_X(LSDA) + 0.72\Delta E_X(Becke88) + 0.81E_C(LYP) + 0.19E_C(VWN)$$

Becke derived the parameters by fitting to a set of thermochemical data, the G1 molecule set. When B3 is paired with a correlation functional other than LYP, the LYP coefficients are retained. Becke also developed a one parameter fit (B). The MPW1PW91 method was developed by Barone and Adamo. It employs a modified PW91 exchange functional with the original PW91 correlation functional and employs a HF to DFT exchange ratio of 0.25:0.75.

Basis Sets

A basis set for computational chemistry is a mathematical expression describing the bounds occupied by an electron. In Hartree-Fock *ab initio* calculations, the orbitals play a direct role in determining the electronic wavefunction. In the Kohn-Sham approach, the orbitals (denoted KS orbitals to distinguish them from their Hartree-Fock counterparts) play only an indirect role in the calculations and serve primarily as a construct to determine the charge density.

Most basis sets use mathematical functions (though some purely numerical basis sets exist such as the one by Delley [42]) to describe an area of space, centred on a nucleus, in which an electron can be found - i.e. a one-electron atomic orbital. The first basis sets developed

used Slater-Type Orbitals (STOs). Problems exist when computing many centre integrals of STOs however as the function used has no analytic derivative, forcing time-consuming numerical computation. To overcome this problem Gaussian-Type Orbitals (GTOs) are commonly adopted. GTOs are much easier to deal with computationally but are less accurate. To compensate for this loss in accuracy, linear combinations of GTOs are employed. The coefficients determining the weighting of each gaussian used are calculated by fitting to a single STO. It typically takes three times the number of GTOs than STOs for a given accuracy. The greater the number of *primitive* gaussians used, the more flexible the expression of the orbital and thus greater accuracy of the calculation. STO-3G is a minimal basis set as it contains only one basis function per atomic orbital. The 3G part indicates that each basis function is a contraction of three primitive gaussians. Minimal basis sets are not recommended for production quality results but are convenient to use in preliminary calculations.

More accuracy can be achieved by representing each orbital by more than one basis function. A *Double ζ (Zeta)* or DZ basis set contains two basis functions per atomic orbital. The Dunning/Huzinaga full double ζ basis set, D95, is of this quality. A Triple Zeta (TZ) basis set uses three basis functions per atomic orbital and so on. It can be rationalised that for most systems, the core electrons do not play a significant role in bonding, thus it is possible to save computer time by treating the core electrons to a lesser accuracy than the valence electrons. A basis set that does this is called a *split-valence* or SV basis set. The smallest example of a split-valence basis set is 3-21G. The 3 indicates that three primitive gaussians are used in the contraction of the core orbitals, 21 indicates that the outer orbitals are split into two functions; *inner* and *outer* functions where the inner function uses two gaussians and the outer function uses only one gaussian. 6-311G is a basis that is triply split, it treats the core only minimally but gives a TZ treatment of the valence electrons. The advantage of using *inner* and *outer* functions for the valence orbitals is that they may change size, growing or shrinking to meet the particular bonding requirements of the molecule.

When bonding occurs in molecules, the atomic orbitals distort away from their idealised shapes. While both split-valence and double- ζ basis set allow orbitals to change size, they do not permit changing of shape. Change of orbital shape can be mimicked by including *polarization functions* to the basis set. These basis functions represent orbitals higher in angular momentum than those occupied in the atom, for example adding *d*-orbitals to a carbon atom whose highest occupied orbitals are *2p*. *d*-functions are used to describe polarisation of *p*-orbitals, *f*-functions are used to describe polarisation of *d*-orbitals and so on. Note that inclusion of *d* and *f* orbitals does not imply that these orbitals are occupied or that they play a significant role in bonding, their inclusion simply increases the accuracy of the electron density around the atom. Polarisation is indicated by either "*" notation or by specifying the orbitals added. In this manner 6-31G(d) and 6-31G* are equivalent. A *DZP* basis set means a double- ζ basis with polarisation functions.

Another way of adding to the basis set to improve accuracy is by the addition of *diffuse* functions. These are necessary to describe weakly-bonded systems such as Hydrogen-bonding and also to describe anions or electronically excited states where the small amount of electron density far from the nucleus plays a significant role. These functions are indicated in a basis set by the prefix *aug-* (abbreviation for augmented) or by a + symbol as in 6-31+G(d,p).

There is a somewhat limited choice of basis sets available for transition metal atoms. Of some 375 basis sets published on EMSL [43], only 55 contain niobium. The third row analogue of niobium, tantalum has only 26 available basis sets. The most commonly employed basis sets for transition metal atoms are the Los Alamos National Laboratory (Lanl) family of basis sets [44–46] and the Stuttgart/Dresden basis set (abbreviated either as SDD or SRSC) [47–49]. Both of these bases are of double- ζ quality.

Effective Core Potentials (ECPs)

In very large systems, such as transition metals that have too many electrons to make regular computation feasible, a more brutal approach can be taken. Considering again, that the core electrons do not play a large part in bonding phenomena, it is possible to treat these electrons as part of the atomic nucleus, in which case they cancel part of the nuclear charge. Some relativistic effects can be taken into account in this process. The resultant quantity is termed an *Effective Core Potential* or ECP.

Computational Method

Previous work [25] established the utility of the B3P86 [50, 51] functional in describing transition metal clusters and it is used for all calculations, except where otherwise specified. The Stuttgart/Dresden (SDD) basis set and associated ECPs were used in all DFT calculations presented in this thesis. Second-row metal atoms had core electrons up to and including the third shell treated by an effective core potential [47–49]. This basis and ECP combination is more commonly referred to as Stuttgart Relativistic Small Core (SRSC) and both terms are used interchangeably. Scalar relativistic effects are accounted for in the ECP, however spin-orbit effects are neglected. Non-metal atoms are treated using the D95 basis set, which is of double- ζ quality.

Roadmap

What follows in this thesis is a series of largely independent “vignettes” or forays into understanding aspects of metal cluster chemistry. Each chapter (except Chapters 4 and 5, which are sequential in theme) may be read independently and each represents a different inroad to an, as yet elusive, full understanding of the relationship between structure and reactivity of

transition metal clusters and how this may be harnessed to efficiently and selectively catalyse chemical reactions.

Chapter 1 explores the reactivity of CO with second-row metal trimers from Nb₃ to Ag₃, for each cluster asking the question, “Does CO bind associatively or dissociatively on this cluster? And why?”. Chapter 2 selects three metal clusters, (Nb₃, Nb₃N₂ and Nb₃C₂) that have been spectroscopically studied and uses multi-reference configuration interaction (MRCI) calculations to investigate the electronic structure of these clusters in some detail. Chapter 3 highlights the difficulty in accurately predicting properties of transition metal clusters and presents a functional tailored to predicting the ionisation potentials of these species. In Chapters 4 and 5, a method of randomly searching configuration space, “Kick” is presented, first focussing on the utility of the original algorithm and then extending it in Chapter 5 to utilise specified chemical fragments. Chapter 6 uses this method to explore the reactivity of CO with another series of transition metal clusters, with Nb₃X stoichiometry.